IEEE Access
Multidisciplinary | Rapid Review | Open Access Journal

Received June 14, 2017, accepted July 4, 2017, date of publication July 18, 2017, date of current version August 22, 2017.

Digital Object Identifier 10.1109/ACCESS.2017.2725269

Static Current Error Elimination Algorithm for Induction Motor Predictive Current Control

XIN-HAI JIN[1], YANG ZHANG[2], AND DIAN-GUO XU[1], (Fellow, IEEE)
[1]Department of Electrical Engineering, Harbin Institute of Technology, Harbin 150001, China
[2]Research and Development Department, Shanghai Sigriner STEP Electric Co., Ltd, Shanghai 201802, China

Corresponding author: Xin-Hai Jin (jinxh@stepelevator.com)

This work was supported by the National Key Technology Research and Development Program of the Ministry of Science and Technology of China under Grant 2014BAF08B05.

ABSTRACT Predictive current control of induction motors can effectively avoid performance deterioration of control caused by delays in the current loop and improve the dynamic performance of current control. However, owing to measurement errors and parameter changes, deviations can appear between the predictive controller parameters and the actual motor parameters. This might lead to static current error, which can cause problems, including decrease in system's efficiency, inability to deliver nominal torque, and to operate in torque control mode, among others. Based on an induction motor model, this paper quantitatively analyzes the influence on current control stability caused by errors in the predictive control model parameters. In addition, we present the mathematical relation between errors in model parameters and static current error, and propose an algorithm to eliminate this type of error. The algorithm corrected the parameters for predictive control using *dq* axis current feedback and eliminated the static error caused by parameter mismatch. Through experimental results, the stability and effectiveness of the proposed method were shown.

INDEX TERMS Static current error elimination, induction motor, parameter correction, predictive current control.

I. INTRODUCTION

Induction motors present advantages such as low cost and high reliability, being widely used in industrial applications. Usually, the complete electrical drive of induction motors considers a cascade control loop, composed of two internal PI-current controllers and one external PI-speed controller. The existence of sampling delays of the digital control system, pulse width modulation (PWM) update delays, dead zone delays, and filter delays, limited the possibility to improve the system dynamic response speed [1].

Using a predictive control algorithm can effectively avoid the deterioration of control performance caused by delays, since it can provide high dynamic performance and low current harmonics [2]–[6].

Predictive current control can be divided into three classes, namely, direct predictive control (DPC), two-configuration predictive control (2PC), and PWM predictive control (PPC). The approach of PPC is sometimes called dead-beat control [7]–[12]. DPC is a direct approach, having the advantage of a fast response on motor stator current, but with the drawback of a high current ripple. PPC largely reduces real-time constraints, has constant switching frequency, and can reduce current ripples. In addition, it can be noted that the detailed method of duty-cycle calculation for PPC is easy to implement without additional sine and cosine computations. The performance of 2PC is similar to PPC, but it presents a higher current ripple [13].

Predictive current control can achieve a good dynamic response of the motor stator current, but still some problems exist. All of the above predictive control schemes rely on the predictive model and the exact knowledge of the electrical parameters of the real motor. However, in a practical situation, errors in parameters measurement probably exist. Moreover, electrical parameters of motors vary during drive operation due to thermal, deep-bar, and saturation effects. Consequently, the difference between model parameters and actual parameters lead to current oscillation or static error. Current oscillation produces mechanical oscillation and drive alarm, whereas static error of current leads to problems such as reducing drive system efficiency, inability to deliver nominal torque under conditions of rated speed, and inability to work in torque control mode. Therefore, it is needed to improve the control algorithm, improve the robustness of predictive current control, and eliminate the static error.

In [15] a robust control method is proposed. This method can prevent current oscillation due to inductance parameter error, but is not able to avoid static current error.

In [16], in order to eliminate the negative effects of parameter errors, PI control is used in the d-axis current, and an integral part is added to the q-axis predictive current control. Although this method is able to eliminate the static current error, the dynamic performance of predictive control is severely weakened by integral saturation effects.

Based on a mathematical model of the induction motor, this paper proposes a novel predictive current control algorithm for induction motors, which quantitative analyzes the influence of parameter errors on the stability of current control. In addition, we present the mathematical relation between model parameter errors and static current error, and present an algorithm to eliminate the static current error.

II. INDUCTION MOTOR MODEL

In the case of indirect vector control, the d-axis reference frame is aligned with the rotor flux. An induction motor stator is classically modeled by a state-space equation, written in the d-q rotor reference frame:

$$\begin{aligned} u_{ds} &= (R_s - \frac{L_s}{L_r}\sigma\omega_{se}^2 T_r^2 R_r) i_{ds} + pL_s i_{ds} - \omega_{re} L_s \sigma i_{qs} \\ u_{qs} &= (R_s + \frac{L_s}{L_r} R_r) i_{qs} + p(L_s - \frac{L_m^2}{L_r}) i_{qs} + \omega_{re} L_s i_{ds}. \end{aligned} \quad (1)$$

In this state-space model, u_{ds} and u_{qs} are, respectively, the d- and q-axis stator voltage, i_{ds} and i_{qs} are, respectively, the d- and q-axis stator currents, R_s is the stator-phase resistance, R_r the rotor-phase resistance, L_s the stator-phase inductance, L_r the rotor-phase inductance, L_m the mutual inductance, p the differential operator, ω_{se} the stator electrical speed, ω_{re} the rotor electrical speed, σ the magnetic leakage factor, $\sigma = 1 - L_m^2/L_s L_r$, and T_r the rotor time constant, $T_r = L_r/R_r$.

For convenience, (1) can be rewritten as

$$p\boldsymbol{i} = \boldsymbol{A}\boldsymbol{i} + \boldsymbol{B}\boldsymbol{u}, \quad (2)$$

where

$$\boldsymbol{i} = \begin{bmatrix} i_{ds} & i_{qs} \end{bmatrix}^T \quad \boldsymbol{u} = \begin{bmatrix} u_{ds} & u_{qs} \end{bmatrix}^T$$

$$\boldsymbol{A} = \begin{bmatrix} -\frac{R_d}{L_s} & \omega_{re}\frac{L_1}{L_s} \\ -\frac{R_q}{L_2} & -\omega_{re}\frac{L_s}{L_2} \end{bmatrix} \quad \boldsymbol{B} = \begin{bmatrix} \frac{1}{L_s} & 0 \\ 0 & \frac{1}{L_2} \end{bmatrix}$$

$$R_d = R_s - \frac{L_s}{L_r}\sigma\omega_{se}^2 T_r^2 R_r \quad R_q = R_s + \frac{L_s}{L_r} R_r$$

$$L_1 = L_s\sigma \quad L_2 = L_s - \frac{L_m^2}{L_r}.$$

III. PWM PREDICTIVE CONTROL

A typical PWM predictive control scheme is shown in Fig. 1. It can be noted that, compared to a classic current control scheme, the PI controller has been replaced by a PWM predictive controller.

If the sampling period T is short enough to consider that the angular rotation during T is negligible, the induction motor

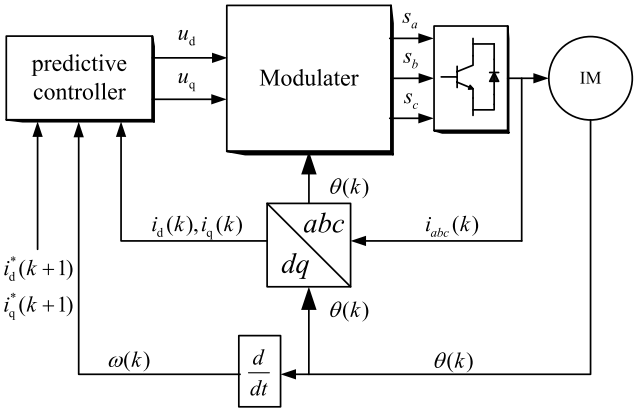

FIGURE 1. Scheme of PWM predictive current control.

can be modeled in discrete time by from (2) using the Euler formula, obtaining

$$\begin{bmatrix} \frac{i_{ds}(k+1) - i_{ds}(k)}{T} \\ \frac{i_{qs}(k+1) - i_{qs}(k)}{T} \end{bmatrix} = \begin{bmatrix} -\frac{R_d}{L_s} & \omega_{re}\frac{L_1}{L_s} \\ -\frac{R_q}{L_2} & -\omega_{re}\frac{L_s}{L_2} \end{bmatrix} \begin{bmatrix} i_{ds}(k) \\ i_{qs}(k) \end{bmatrix} + \begin{bmatrix} \frac{1}{L_s} & 0 \\ 0 & \frac{1}{L_2} \end{bmatrix} \begin{bmatrix} u_{ds}(k) \\ u_{qs}(k) \end{bmatrix}, \quad (3)$$

where $i_{ds}(k+1)$ and $i_{qs}(k+1)$ are, respectively, the d- and q-axis reference stator currents at time $k+1$, $i_{ds}(k)$ and $i_{qs}(k)$ are, respectively, the d- and q-axis actual stator currents at time k.

From (3), we deduce the stator current difference equations

$$\begin{bmatrix} i_{ds}(k+1) \\ i_{qs}(k+1) \end{bmatrix} = \begin{bmatrix} 1 - \frac{R_d T}{L_s} & \omega_{re}\frac{L_1 T}{L_s} \\ 1 - \frac{R_q T}{L_2} & -\omega_{re}\frac{L_s T}{L_2} \end{bmatrix} \begin{bmatrix} i_{ds}(k) \\ i_{qs}(k) \end{bmatrix} + \begin{bmatrix} \frac{T}{L_s} & 0 \\ 0 & \frac{T}{L_2} \end{bmatrix} \begin{bmatrix} u_{ds}(k) \\ u_{qs}(k) \end{bmatrix} \quad (4)$$

and then obtain the stator voltages

$$\begin{bmatrix} u_{ds}(k) \\ u_{qs}(k) \end{bmatrix} = \begin{bmatrix} \frac{L_s}{T} & 0 \\ 0 & \frac{L_2}{T} \end{bmatrix} \begin{bmatrix} i_{ds}(k+1) \\ i_{qs}(k+1) \end{bmatrix} + \begin{bmatrix} R_d - \frac{L_s}{T} & -\omega_{re} L_1 \\ \omega_{re} L_s & R_q - \frac{L_2}{T} \end{bmatrix} \begin{bmatrix} i_{ds}(k) \\ i_{qs}(k) \end{bmatrix}. \quad (5)$$

A space vector PWM generator is used to translate $u_{ds}^*(k)$ and $u_{qs}{}^*(k)$ into switching signals that are then applied to an inverter switch generator. Ideally, at time $k+1$, currents

$i_{ds}(k+1)$ and $i_{qs}(k+1)$ will be equal to the reference currents $i_{ds}^*(k)$ and $i_{qs}{}^*(k)$, respectively. Therefore, based on the discrete-time model in (5), the reference voltage vector is obtained as

$$\begin{bmatrix} u_{ds}^*(k) \\ u_{qs}{}^*(k) \end{bmatrix} = \begin{bmatrix} \frac{L_s}{T} & 0 \\ 0 & \frac{L_2}{T} \end{bmatrix} \begin{bmatrix} i_{ds}^*(k) \\ i_{qs}{}^*(k) \end{bmatrix} + \begin{bmatrix} R_d - \frac{L_s}{T} & -\omega_{re}L_1 \\ \omega_{re}L_s & R_q - \frac{L_2}{T} \end{bmatrix} \begin{bmatrix} i_{ds}(k) \\ i_{qs}(k) \end{bmatrix}, \quad (6)$$

where $i_{ds}^*(k)$ and $i_{qs}{}^*(k)$ are, respectively, the d- and q-axis reference stator currents at time k, $u_{ds}^*(k)$ and $u_{qs}{}^*(k)$ are, respectively, the d- and q-axis stator voltage reference at time k.

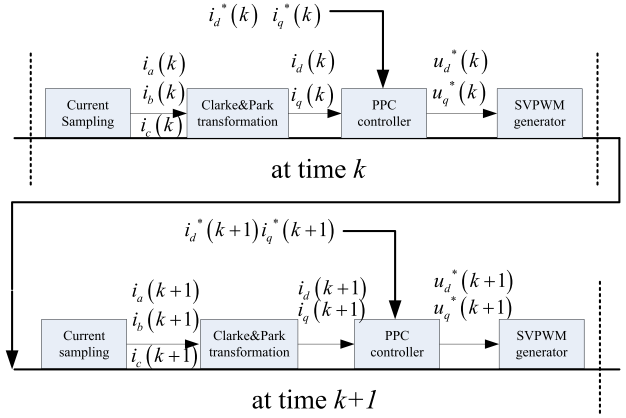

FIGURE 2. Operation principle of PPC.

The basic operating principle of PPC is shown in Fig. 2. Here, the currents $i_{ds}(k)$ and $i_{qs}(k)$ are different to the corresponding reference currents $i_{ds}^*(k)$ and $i_{qs}{}^*(k)$ at time k. This error is used to calculate the reference voltages $u_{ds}^*(k)$ and $u_{qs}{}^*(k)$ in (6), which are applied to the load at time k.

IV. ERROR ANALYSIS OF MODEL PARAMETERS

A. INFLUENCE OF PARAMETER L_2 ERROR ON STABILITY

Usually, the parameter L_2 of a predictive current controller differs from the actual parameter of the motor. In this section, we denote L_2 as the motor actual inductance and $L_2\prime$ as the predictive current controller inductance. Then, by replacing L_2 with $L_2\prime$ in (6) we have

$$u_{qs}{}^*(k) = \frac{L_2'}{T} i_{qs}{}^*(k+1) + (R_q - \frac{L_2'}{T}) i_{qs}(k) + \mathrm{L_s}\omega_{\mathrm{re}} i_{ds}(k). \quad (7)$$

Ideally, $u_{qs}{}^*(k) = u_{qs}(k)$; hence,

$$\frac{L_2}{T} i_{qs}(k+1) + (R_q - \frac{L_2}{T}) i_{qs}(k) + \mathrm{L_s}\omega_{\mathrm{re}} i_{ds}(k) = \frac{L_2'}{T} i_{qs}{}^*(k+1) + (R_q - \frac{L_2'}{T}) i_{qs}(k) + \mathrm{L_s}\omega_{\mathrm{re}} i_{ds}(k). \quad (8)$$

Then, the difference equation for the q-axis stator current is

$$i_{qs}(k+1) = \frac{L_2'}{L_2} i_{qs}{}^*(k+1) + \frac{L_2 - L_2'}{L_2} i_{qs}(k). \quad (9)$$

The transformation of (9) into a discrete domain transfer function is as follows

$$\frac{i_{qs}(z)}{i_{qs}{}^*(z)} = \frac{L_2'}{L_2} \frac{z}{z - (1 - L_2'/L_2)}, \quad (10)$$

and the characteristic root of this system is obtained as

$$z = 1 - L_2'/L_2. \quad (11)$$

When the pole is within the Z plane unit circle, i.e., $0 < L_2\prime < 2L_2$, the discrete control system can be kept stable, since usually, the error between parameters should be limited to two times.

B. INFLUENCE OF PARAMETER L_2 ERROR ON STATIC CURRENT ERROR

In this section Δi_{qs} is the static error of q-axis current i_{qs}, i.e., the difference between i_{qs} and $i_{qs}{}^*$:

$$\Delta i_{qs}(k+1) = i_{qs}{}^*(k+1) - i_{qs}(k+1). \quad (12)$$

From (9) and (12) we obtain

$$\Delta i_{qs}(k+1) = \frac{L_2 - L_2'}{L_2'} [i_{qs}(k+1) - i_{qs}(k)]. \quad (13)$$

Obviously, since the control sampling period is very short, we can consider the difference between $i_{qs}(k+1)$ and $i_{qs}(k)$ as being $i_{qs}(k+1) - i_{qs}(k) \approx 0$; therefore, the influence of the parameter error on the static current error is negligible.

C. INFLUENCE OF PARAMETER R_q ERROR ON STABILITY

Usually, the parameter R_q of a predictive current controller is different to the actual motor parameter. In this section, we denote R_q as actual resistance of motor and $R_q{}'$ as the predictive current controller resistance. Then, by replacing R_q with $R_q{}'$ in (6), we obtain

$$u_{qs}{}^*(k) = \frac{L_2}{T} i_{qs}{}^*(k+1) + (R_q{}' - \frac{L_2}{T}) i_{qs}(k) + \mathrm{L_s}\omega_{\mathrm{re}} i_{ds}(k). \quad (14)$$

Ideally, $u_{qs}{}^*(k) = u_{qs}(k)$ and from (6) and (14), we obtain

$$i_{qs}(k+1) = i_{qs}{}^*(k+1) + \frac{T}{L_2}(R_q' - R_q) i_{qs}(k), \quad (15)$$

whose Z transform is

$$\frac{i_{qs}(z)}{i_{qs}{}^*(z)} = \frac{L_2'}{L_2} \frac{z}{z - \frac{T}{L_2}(R_q{}' - R_q)}. \quad (16)$$

When the pole is within the Z plane unit circle, i.e., $R_q - L_2/T < R_q{}' < R_q + L_2/T$, the discrete control system can be kept stable.

D. INFLUENCE OF PARAMETER R_q ERROR ON STATIC CURRENT ERROR

From (12) and (15) we obtain

$$\Delta i_{qs}(k+1) = \frac{T}{L_2} i_{qs}(k) \Delta R_q, \tag{17}$$

where $\Delta R_q = R_q - R_q'$, and $\Delta i_{qs}(k+1)$ is proportional to $i_{qs}(k)$ and ΔR_q. On the other hand, when $i_{qs}(k)$ is close to zero, i.e., the motor is at no load operation, $\Delta i_{qs}(k+1)$ is also close to zero. In other words, when the motor is at no load operation, even if the actual current is different to the reference current, this does not depend on the parameter R_q error.

TABLE 1. Parameter *R*Q error and current error.

	$R_q > R_q'$	$R_q < R_q'$
$i_{qs} > 0$	$i_{qs}^* > i_{qs}$	$i_{qs}^* < i_{qs}$
$i_{qs} < 0$	$i_{qs}^* < i_{qs}$	$i_{qs}^* > i_{qs}$

When i_{qs} is positive, if parameter R_q' of the predictive controller is less than actual parameter R_q, then Δi_{qs} is positive, i.e., the actual current i_{qs} is less than the reference current i_{qs}^*; if parameter R_q' of the predictive controller is greater than actual parameter R_q, then Δi_{qs} is negative, i.e., the actual current i_{qs} is greater than reference current i_{qs}^*. Under conditions of negative i_{qs}, the relationship between the static current error and the parameter error is converse as shown in Table 1.

E. INFLUENCE OF PARAMETER L_s ERROR ON STABILITY

Now we consider the case that parameter L_s of predictive current controller is different to the actual motor parameter. In this sectiončwe denote L_s as the actual motor inductance, $L_s\prime$ as the predictive current controller inductance, and define $\Delta L_s = L_s - L_s'$. Then, by replacing L_s by $L_s\prime$ in (6), we obtain

$$i_{qs}(k+1) = i_{qs}^*(k+1) + \frac{T}{L_2}(L_s' - L_s)\omega_{re} i_{ds}(k). \tag{18}$$

It can be seen from (18) that a deviation of L_s will not cause i_{qs} to be out of control; in other words, even if the deviation of Ls is large, current i_{qs} will not oscillate

F. INFLUENCE OF PARAMETER L_s ERROR ON STATIC CURRENT ERROR

From (12) and (18), we obtain

$$\Delta i_{qs}(k+1) = \Delta L_s \frac{T}{L_2} \omega_{re} i_{ds}(k). \tag{19}$$

Thus, $\Delta i_{qs}(k+1)$ is proportional to ΔL_s, ω_{re}, and $i_{ds}(k)$.

When the motor runs forward (i.e., $\omega_{re} > 0$), if parameter $L_s\prime$ of predictive controller is less than actual L_s, then Δi_{qs} is positive, i.e., actual current i_{qs} is less than reference current i_{qs}^*; if parameter $L_s\prime$ of predictive controller is greater than actual L_s, then Δi_{qs} is negative, i.e., actual current i_{qs} is greater than reference current i_{qs}^*. Under conditions of motor backward rotation, the relationship between current static error and parameter error is converse, as shown in Table 2.

TABLE 2. Parameter *Ls* error and current error.

	$L_s > L_s'$	$L_s < L_s'$
$\omega_{re} > 0$	$i_{qs}^* > i_{qs}$	$i_{qs}^* < i_{qs}$
$\omega_{re} < 0$	$i_{qs}^* < i_{qs}$	$i_{qs}^* > i_{qs}$

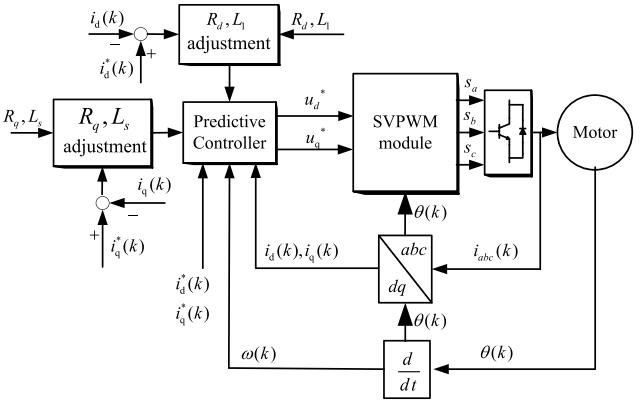

FIGURE 3. Predictive current control with static error elimination algorithm.

In principle, the upper and lower parts of (6) are the same, L_1 in (6) corresponds to L_s in sections E and F, R_d in (6) corresponds to R_q in sections C and D, L_s in the upper part of (6) corresponds to L_2 in sections A and B, so the derivation using L_1, R_d, and L_s will not be repeated here.

G. STATIC CURRENT ERROR ELIMINATION

In summary, error of parameters L_s' and R_q' of the predictive controller can cause static current error Δi_{qs}. When the motor runs at no load operation, static current error Δi_{qs} is caused by a deviation of parameter L_s' and not by parameter R_q'.

In this paper, we used (20) when the motor ran in no load operation, then adjusted the parameter L_s' of the predictive controller through the static current error Δi_{qs}, to finally obtain a convergence of parameter L_s' of the predictive controller to the actual value, in order to eliminate the static current error Δi_{qs}. Equation (20) is given by

$$L_{sf} = L_s' + K_{iL} \sum_{n}^{k} [i_{qs}^*(n) - i_{qs}(n)], \tag{20}$$

where L_{sf} is the final convergence of parameter L_s of predictive controller; L_s' is the initial value of the predictive controller, i.e., it is the unadjusted value of parameter L_s; and K_{iL} is an integral factor.

After parameter L_s finally converges to the actual value, with the motor running in stable load operation, if there is still static current error Δi_{qs}, then it is caused by deviation of parameter R_q'. We used (21) when the motor ran in stable load operation, through the static current error Δi_{qs} to adjust parameter R_q' of the predictive controller, until it is finally converged to the actual value. The equation we used is

FIGURE 4. Setup of the test platform.

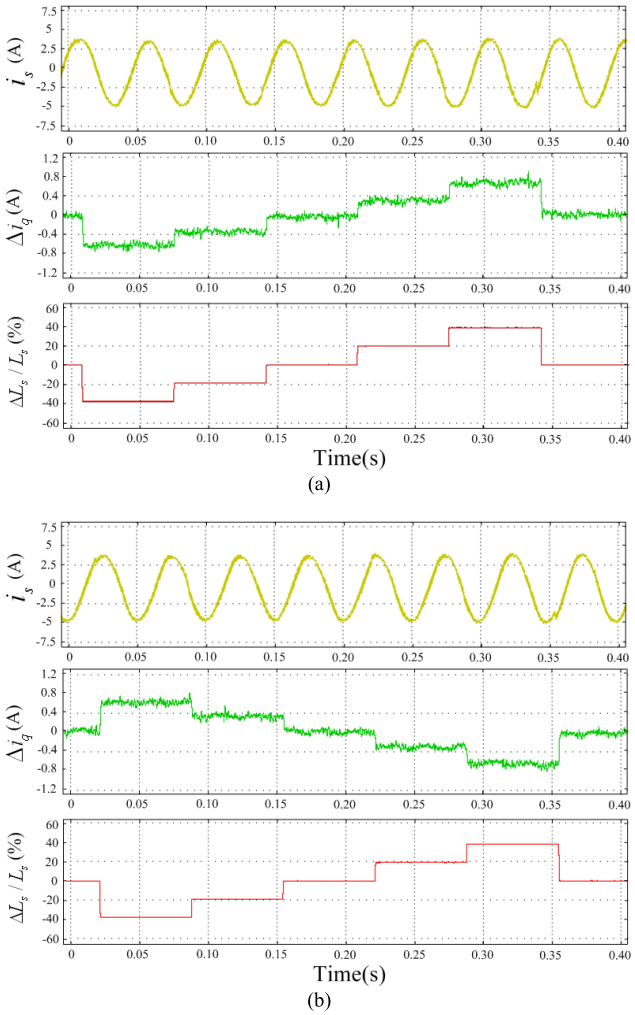

FIGURE 5. Static current error and parameter error ΔL_s. (a) Motor rotates forward, (b) motor rotates backwards.

given by

$$R_{qf} = R_q{}' + K_{iR} \sum_{n}^{k} [i_{qs}{}^*(n) - i_{qs}(n)], \tag{21}$$

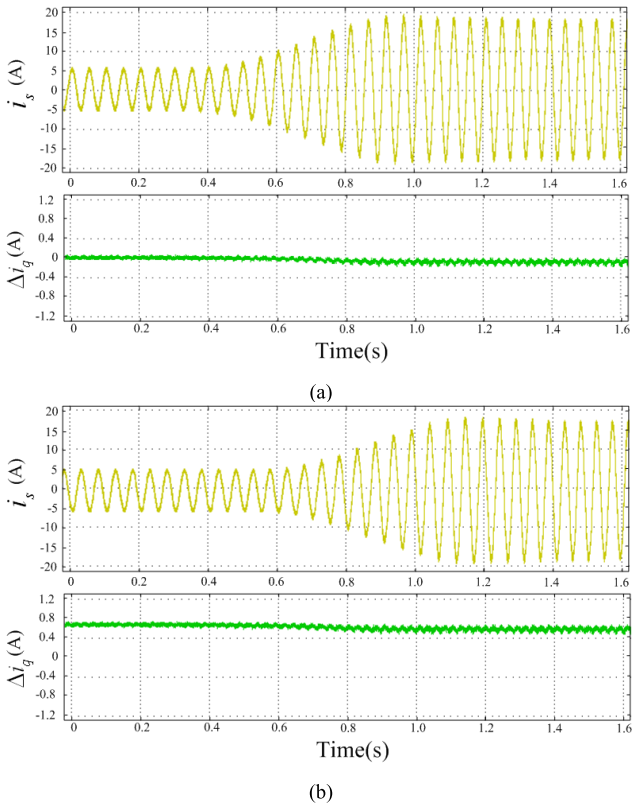

FIGURE 6. Static current error and motor load for (a) $\Delta L_s = 0$ and (b) $\Delta L_s = 40\%\ L_s$.

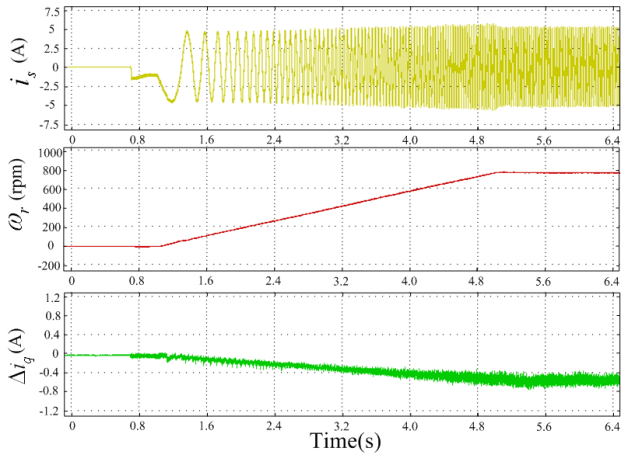

FIGURE 7. Static current error and motor speed.

where R_{qf} is the final convergence of parameter R_q of the predictive controller; $R_q{}'$ is the initial value of parameter R_q, i.e., it is the unadjusted value of parameter R_q; and K_{iR} is an integral factor.

A diagram of the predictive current controller with static error elimination is shown in Fig. 3.

When the parameters L_{sf} and R_{qf} of the predictive controller are equal to the actual parameters of the motor, the static current error is eliminated. Considering that a sudden change of current i_{qs} has led to a change of parameters L_{sf} and R_{qf}, it is necessary to avoid adjusting these

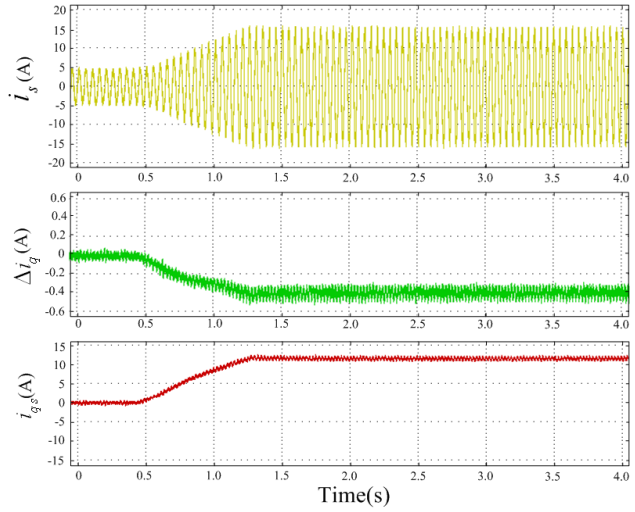

FIGURE 8. Static current error and motor load when $\Delta R_q = -100\% R_q$.

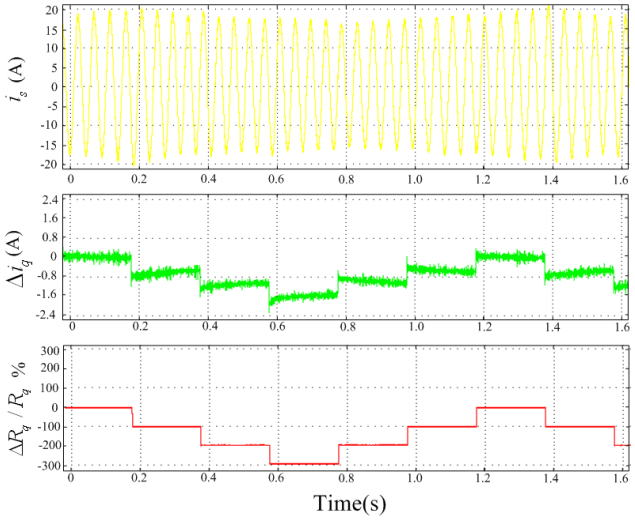

FIGURE 9. Static current error and parameter error ΔR_q.

parameters during the transient operation of motor. Instead, parameter L_{sf} should be adjusted while the motor is running in stable no load operation, whereas parameter R_{qf} should be adjusted while the motor is running in stable load operation.

V. EXPERIMENTAL RESULTS

In this paper, the proposed PPC is experimentally tested on an inverter-fed induction motor drive platform. The control and system parameters are shown in Table 3; the frequency of STM32F103 board, which was the inverter CPU was of 72 MHz. Fig. 4 shows the setup of the test platform.

Experimental results are shown in Fig. 5 to Fig. 13, i_s is the motor stator current, Δi_q is the static error of q-axis current i_{qs}, $\Delta L_s/L_s$ is the ratio between the parameter L_s deviation and the actual value. Fig. 5a) shows the results under no load condition, with the motor rotating forward at 40% of the rated speed, the d-axis current i_d remains at 3.78 A, and the parameter L_s' of the predictive current controller is set to 140%, 120%, 100%, 80%, and 60% of

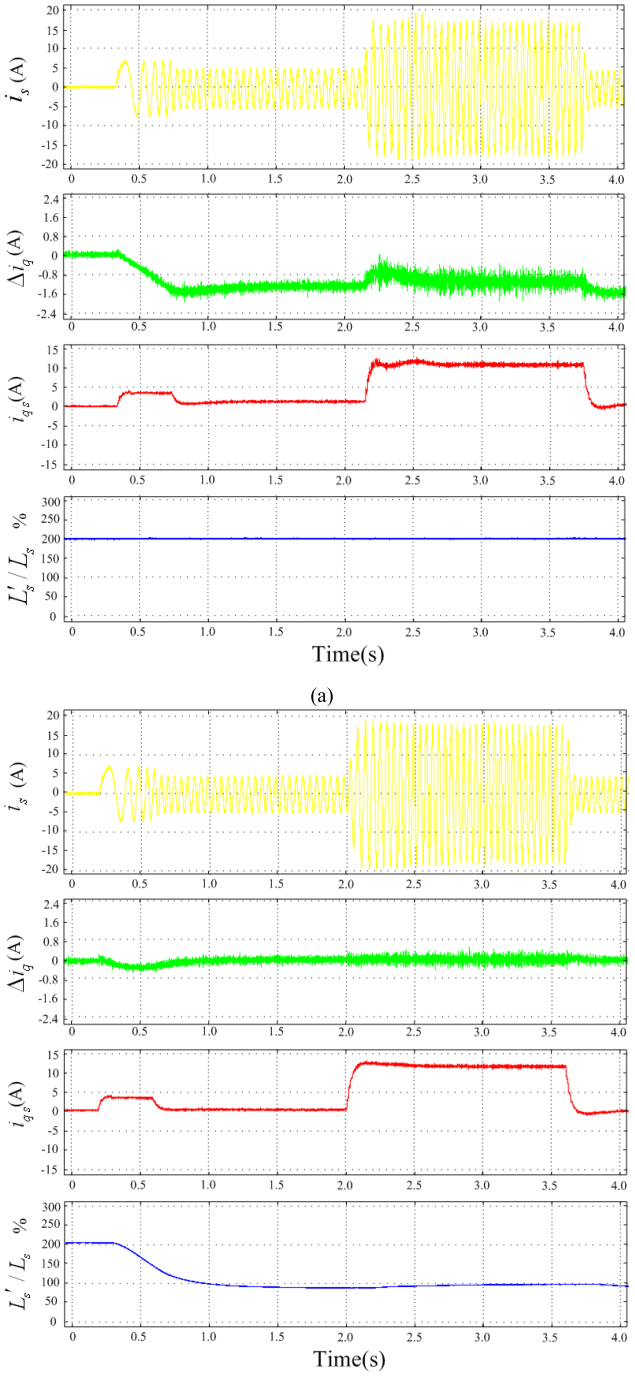

FIGURE 10. Predictive control parameter L_s' correction when (a) $L_s'=2L_s$ with no correction and (b) $L_s'=2L_s$ with correction.

the actual motor parameter L_s, i.e., ΔL_s is -40%, -20%, 0%, 20%, and 40%, respectively, whereas the remaining predictive controller parameters are consistent with the actual motor parameters. Fig. 5(a) shows that the static error of q-axis current is proportional to the deviation of the parameter L_s, when the speed is constant. In Fig. 5(b), the motor rotates backwards, whereas the other experimental conditions are the same as in Fig. 5(a). Fig. 5(a) and Fig. 5(b) present opposite

TABLE 3. Ratings and parameters of the motor.

Parameter	Value	Unit
Rated power P_e	5.5	kW
Rated voltage U_e	380	V
Rated current I_e	12.6	A
Rated frequence f_e	50	Hz
Rated speed n_e	960	rpm
Number of poles pairs z_p	3	
Stator resistance R_s	0.842	Ω
Rotor resistance R_r	0.535	Ω
Stator inductance L_s	111.2	mH
Rotor inductance L_r	111.2	mH
Mutual inductance L_m	107.9	mH

behaviors, since for the same values of $\Delta L_s/L_s$, the absolute value of the static current error is the same, but the sign of the error is opposite, which is consistent with (19).

Fig. 6(a) shows the results under no load condition, with the motor rotating forward at 40% of the rated speed, the d-axis current i_d remains at 3.78 A, and the parameter $L_s{}'$ of the predictive current controller is consistent with the actual parameter L_s. In Fig. 6(b), parameter $L_s{}'$ is 60% of actual parameters L_s, with the other experimental conditions being the same as in Fig. 6(a). When the motor load increases gradually from no load to rated load, in Fig. 6(a) Δi_q remains zero, whereas in Fig. 6(b) Δi_q remains at 0.65 A. The experimental results show that, no matter whether parameter $L_s{}'$ is consistent with the actual parameter L_s, Δi_q will not change with q-axis current i_q, in other words, Δi_q does not vary with the motor load.

In Fig. 7 under the no load condition, the motor speed increases from zero to 800 rpm and parameter $L_s{}'$ is 80% of L_s. It can be seen that the increase of motor speed produces and increase in the current static error.

In Fig. 8, parameter $R_q^{'}$ is 200% of R_q, the motor remains at 40% of the rated speed, and the motor load gradually increases from 0% to 100% of the rated load. Again, an increase in the motor load produces an increase the static current error, which is consistent with (17).

In Fig. 9, under rated load condition, the motor rotates forward at 40% of the rated speed, parameter $R_q{}'$ is 100%, 200%, 300%, and 400% of R_q, i.e., $\Delta R_q/R_q$ is 0%, −100%, −200%, and −300%, respectively, whereas the other predictive controller parameters are consistent with the actual motor parameters. The ratio $\Delta R_q/R_q$ describes the relation between the deviation of parameter $R_q{}'$ and the actual value. Fig. 9 shows that current static error Δi_q is proportional to ΔR_q, which is consistent with (19).

In Fig. 10 to Fig. 13, the motor operation and the load conditions are the same, described as follows. Under no load

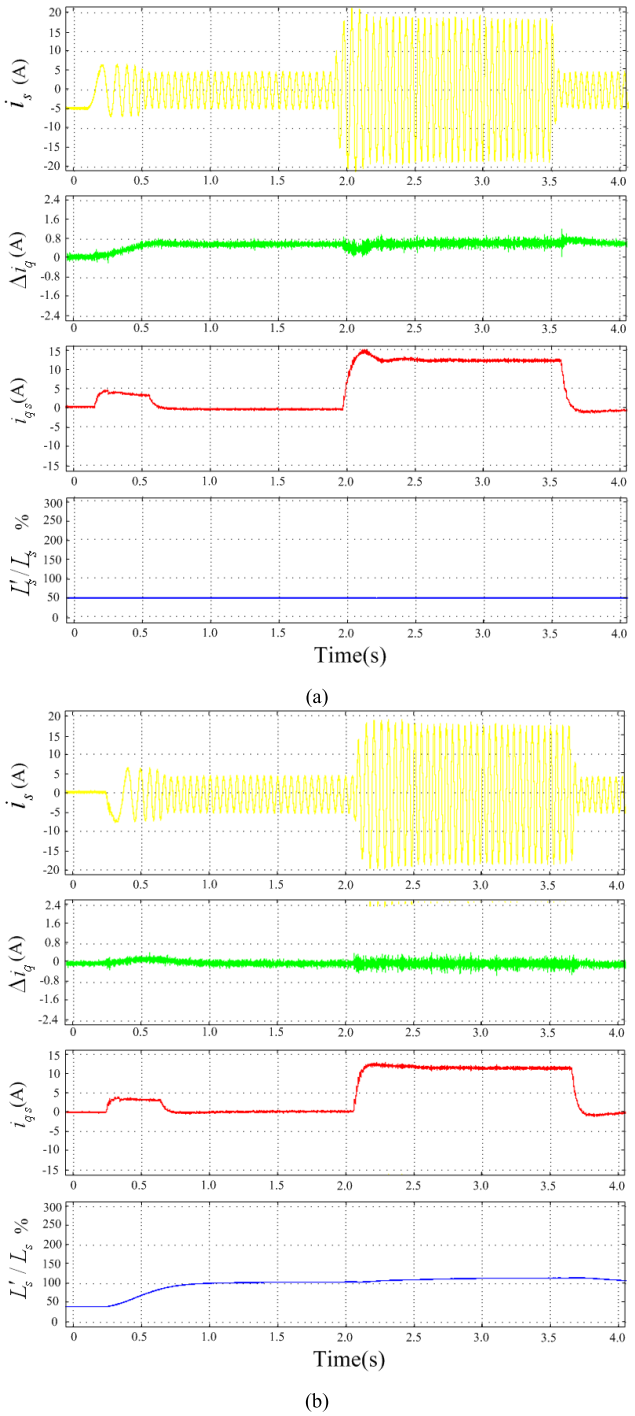

FIGURE 11. Predictive control parameter $L_s{}'$ correction when (a) $L_s{}' = 0.5L_s$ with no correction and (b) $L_s{}' = 0.5L_s$ with correction.

condition, the motor goes from zero to 40% of the rated speed in 0.4 s and then it rotates at a constant speed with and instant 100% of the rated load on motor during 1.5 s, followed by a sudden unload.

In Fig. 10(a), parameter $L_s{}'$ remains constant at 200% of the actual motor parameter L_s, whereas in Fig. 10(b), parameter $L_s{}'$ is gradually adjusted from 200% of L_s to L_s according to (20).

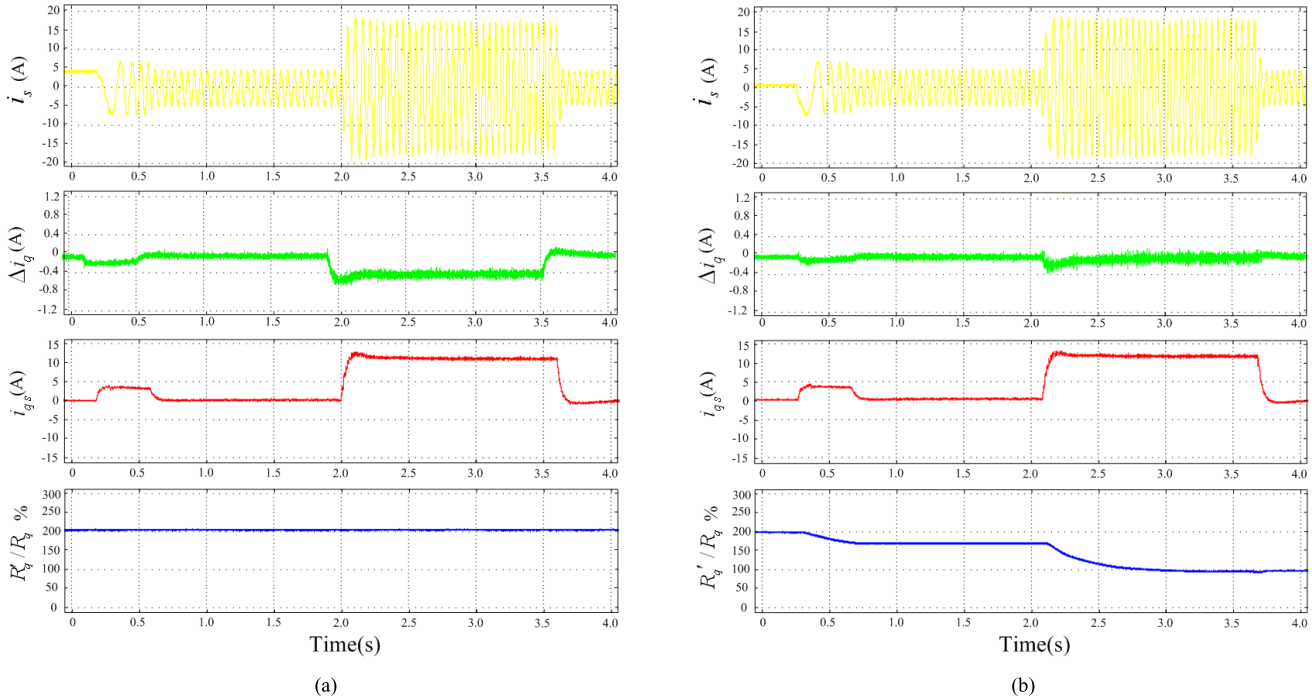

FIGURE 12. Predictive control parameter R_q' correction when (a) $R_q' = 2R_q$ with no correction and (b) $R_q' = 2R_q$ with correction.

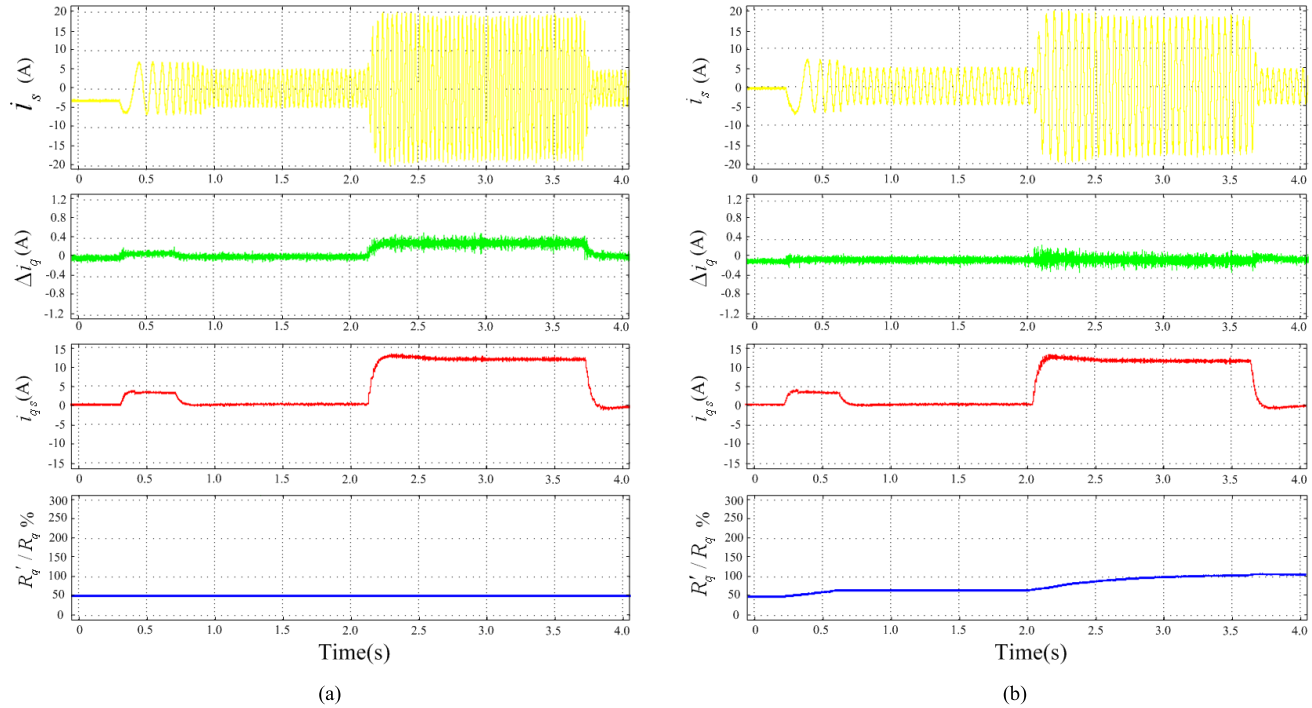

FIGURE 13. Predictive control parameter R_q' correction when (a) $R_q' = 0.5$Rq with no correction and (b) $R_q' = 0.5R_q$ with correction.

In Fig. 10(a), Δi_q is zero with null motor speed, remains proportional to the motor speed, and does not depend on i_q. In Fig. 10(b), the initial condition of L_s' is 200% of L_s, with the acceleration of the motor, L_s' gradually decreases, and approximately after 0.7 s L_s' reaches the value of L_s and remains within a small range of fluctuation from that value. In the motor acceleration, despite of a decrease in L_s', the motor speed increases fast, producing an increase in Δi_q.

However, the amplitude variation of Δi_q in Fig. 10(b) is much smaller than that in Fig. 10(a).Afterwards, Ls' continues to decrease and Δi_q also decreases, until L_s' reaches the value of L_s, when Δi_q goes to zero.

In Fig. 11(a), parameter $L_s{}'$ remains at 50% of the actual motor parameter L_s, whereas in Fig. 11(b), parameter $L_s{}'$ is gradually adjusted from 50% of L_s to L_s according (20). The waveforms of Fig. 10 and Fig. 11 are opposite; hence, these will not be repeated here.

In Fig. 12(a), parameter $R_q{}'$ remains at 200% of the actual motor parameter R_q, whereas in Fig. 12(b), parameter $R_q{}'$ is gradually adjusted from 200% of R_q to 100% R_q according to (21). Except from $R_q{}'$, the other parameters of the predictive current controller are consistent with the actual parameters.

In Fig. 12(a), when the motor has no load, Δi_q is zero and remains proportional to q-axis current i_q, whereas Δi_q does not depend on motor speed. In Fig. 12(b), within the first 0.4 s, the motor accelerates and i_q remains at 3.0 A, whereas $R_q{}'$ decreases slowly. Afterwards, the motor rotates at constant speed, but $R_q{}'$ does not converge to R_q because i_q is close to 0 and, consequently, $R_q{}'$ stops converging. On the other hand, when the motor load suddenly increases, i_q increases rapidly to 12.8 A, $R_q{}'$ continues decreasing and eventually converges to the actual value of R_q, and remains in that value within a small range of fluctuation. The reduction of $R_q{}'$ produces a decrease in Δi_q until it reaches zero.

In Fig. 13(a), parameter $R_q{}'$ remains at 50% of the actual motor parameter R_q, whereas in Fig. 13(b), parameter $R_q{}'$ is gradually increased from 50% of R_q to 100% of R_q according to (21). The waveform of Fig. 12 and Fig. 13 are opposite; hence, these will not be repeated here.

VI. CONCLUSION

When the model parameters of predictive current controller are different from the actual motor parameters, a negative impact on the control performance appears, leading to static current error between the reference current and the actual current. In this study, we proposed an error correction method applied to predictive current control for induction motors that could effectively eliminate the static current error. Experimental results verified the feasibility and effectiveness of this method.

REFERENCES

[1] D. Casadei, F. Profumo, G. Serra, and A. Tani, "FOC and DTC: Two viable schemes for induction motors torque control," *IEEE Trans. Power Electron.*, vol. 17, no. 5, pp. 779–787, Sep. 2002.
[2] E. S. de Santana, E. Bim, and W. C. do Amaral, "Predictive algorithm for controlling speed and rotor flux of induction motor," *IEEE Trans. Ind. Electron.*, vol. 55, no. 12, pp. 4398–4407, Dec. 2008.
[3] P. Cortés, M. P. Kazmierkowski, R. M. Kennel, D. E. Quevedo, and J. Rodríguez, "Predictive control in power electronics and drives," *IEEE Trans. Ind. Electron.*, vol. 55, no. 12, pp. 4312–4324, Dec. 2008.
[4] J. Rodriguez, R. M. Kennel, J. R. Espinoza, M. Trincado, C. A. Silva, and C. A. Rojas, "High-performance control strategies for electrical drives: An experimental assessment," *IEEE Trans. Ind. Electron.*, vol. 59, no. 2, pp. 812–820, Feb. 2012.
[5] M. R. Arahal, F. Barrero, S. Toral, M. Duran, and R. Gregor, "Multi-phase current control using finite-state model-predictive control," *Control Eng. Pract.*, vol. 17, no. 5, pp. 579–587, 2009.
[6] F. Barrero, M. R. Arahal, R. Gregor, S. Toral, and M. J. Duran, "A proof of concept study of predictive current control for VSI-driven asymmetrical dual three-phase AC machines," *IEEE Trans. Ind. Electron.*, vol. 56, no. 6, pp. 1937–1954, Jun. 2009.
[7] I. Sarasola, J. Poza, M. A. Rodríguez, and G. Abad, "Predictive direct torque control for brushless doubly fed machine with reduced torque ripple at constant switching frequency," in *Proc. IEEE ISIE*, Jun. 2007, pp. 1074–1079.
[8] V. Ambrozic, D. Nedeljkovic, and M. Nemec, "Predictive torque control of induction machines using immediate flux control," in *Proc. IEEE Int. Conf. Elect. Mach. Drives*, San Antonio, TX, USA, May 2005, pp. 565–571.
[9] V. Ambrozic, R. Fiser, and D. Nedeljkovic, "Direct current control-A new current regulation principle," *IEEE Trans. Power Electron.*, vol. 18, no. 1, pp. 495–503, Jan. 2003.
[10] P. Correa, M. Pacas, and J. Rodriguez, "Predictive torque control for inverter-fed induction machines," *IEEE Trans. Ind. Electron.*, vol. 54, no. 2, pp. 1073–1079, Apr. 2007.
[11] G. Gatto, I. Marongiu, A. Serpi, and A. Perfetto, "Predictive control of synchronous reluctance motor drive," in *Proc. IEEE ISIE*, Jun. 2007, pp. 1147–1152.
[12] H.-T. Moon, H.-S. Kim, and M.-J. Youn, "A discrete-time predictive current control for PMSM," *IEEE Trans. Power Electron.*, vol. 18, no. 1, pp. 464–472, Jan. 2003.
[13] F. Morel, X. Lin-Shi, J. M. Retif, B. Allard, and C. Buttay, "A comparative study of predictive current control schemes for a permanent-magnet synchronous machine drive," *IEEE Trans. Ind. Electron.*, vol. 56, no. 7, pp. 2715–2728, Jul. 2009.
[14] P. Wipasuramonton, Z. Q. Zhu, and D. Howe, "Predictive current control with current-error correction for PM brushless AC drives," *IEEE Trans. Ind. Appl.*, vol. 42, no. 4, pp. 1071–1079, Jul. 2006.
[15] L. Niu, M. Yang, K. Liu, and D. Xu, "A predictive current control scheme for permanent magnet synchronous motors," in *Proc. CSEE*, 2012, vol. 32. no. 6, pp. 132–135.
[16] W. H. Wang and X. Xiao, "Adaptive incremental predictive control method for current of PMSM based on online identification of inductance," *Electr. Mach. Control*, vol. 18, no. 2, pp. 76–81, 2014.

XIN-HAI JIN was born in Shandong, China, in 1974. He received the B.S. degree in automation from Qingdao University, Qingdao, China, in 2001, and the M.S. degree in control engineering from Tongji University, Shanghai, China, in 2010. He is currently pursuing the Ph.D. degree in electrical engineering from the Harbin Institute of Technology, Harbin, China.

His research interests include high-power electronics, inverter drive system, control algorithms, and PWM techniques.

YANG ZHANG was born in Liaoning, China, in 1984. He received the B.S. and M.S. degrees in electrical engineering from the Harbin Institute of Technology, Harbin, China, in 2007 and 2009 respectively. He is currently with Shanghai Sigriner STEP Electric Co., Ltd, Shanghai, China.

His research interests include digital control of power converters, control algorithms, and induction machine drives.

DIAN-GUO XU (M'97–SM'12–F'17) received the B.S. degree in control engineering from Harbin Engineering University, Harbin, China, in 1982, and the M.S. and Ph.D. degrees in electrical engineering from the Harbin Institute of Technology (HIT), Harbin, in 1984 and 1989, respectively. In 1984, he joined as an Assistant Professor with the Department of Electrical Engineering, HIT, where he has been a Professor since 1994. He was the Dean of School of Electrical Engineering and Automation, HIT, from 2000 to 2010. He is currently the Vice President of HIT. He authored over 600 technical papers. His research interests include renewable energy generation technology, power quality mitigation, sensorless vector controlled motor drives, and high performance PMSM servo system.

Dr. Xu is currently an Associate Editor of the IEEE Transactions on Industrial Electronics and the IEEE Journal of Emerging and Selected Topics in Power Electronics. He serves as the Chairman of the IEEE Harbin Section.